X-523-65-199

NASA TMX-55225

SIGNAL LEVEL PERFORMANCE OF THE INTERFEROMETER RE-ENTRY TRACKER

BY
V. R. SIMAS

MAY 10, 1965

NASA — GODDARD SPACE FLIGHT CENTER
GREENBELT, MARYLAND

SIGNAL LEVEL PERFORMANCE OF THE INTERFEROMETER RE-ENTRY TRACKER

by
V. R. Simas

May 10, 1965

Goddard Space Flight Center
Greenbelt, Maryland

SIGNAL LEVEL PERFORMANCE OF THE INTERFEROMETER RE-ENTRY TRACKER

by

V. R. Simas

SUMMARY

27363

The received signal levels, P_r, are derived as a function of spacecraft position relative to the Re-entry ship. Plots of P_r vs time are included for the pertinent re-entry trajectories and the maximum deviations in spacecraft attitude, i.e., 20° lift, horizontal, and 20° drag. The factors comprising the conventional far-field equation are discussed and the criteria established for the assumptions in the values of particular parameters that were used. The results show that with 14 watts being radiated from the re-entering Apollo spacecraft, and limited by either radio blackout and/or 10° elevation angles, the observation tracking periods are nominally 100 seconds. These periods drop only about 10% with the introduction of losses amounting to 10 db. With 20 db of losses the tracking periods are nominally 70 seconds. An additional 7 db of sensitivity is obtained when phase lock-up is established. With this 27 db margin (about 10 db must be allocated the spacecraft) and the possibility of even longer observation periods due to possible interferometer operation below 10°, the application of the Interferometer Re-entry Tracker is considered appropriate for meeting the passive acquisition requirements associated with the Apollo Re-entry Program.

author

CONTENTS

LIST OF ILLUSTRATIONS

SIGNAL LEVEL PERFORMANCE OF THE INTERFEROMETER RE-ENTRY TRACKER

INTRODUCTION

As discussed in detail in Dr. F. O. Vonbun's report "Re-entry Tracking for Apollo",[1] the Apollo spacecraft, during its re-entry phase, has the capability of flying a variety of trajectories after it enters the earth's atmosphere. Because of interruption of radio contact caused by the radio blackout problem a positive means of signal acquisition is necessary after blackout terminates.

A simple five-element broad beam radio interferometer has been proposed as applicable in satisfying the signal acquisition requirements. This system is described in GSFC report X-523-63-56, "A System for Re-entry Tracking of the Apollo Spacecraft".[2] The feasibility of this approach has been demonstrated by such a system developed at GSFC. Final quantitative measurements on the performance of the system will be made during the summer of 1965.

The purpose of this report is to show the variations in signal level received by the radio interferometer system for various trajectories and attitudes of the re-entering Apollo Command Module. Since the operational success of this acquisition system largely depends upon the length of the observational period, the received signal level, P_r, is plotted against time. The results, shown in Figure 1 clearly reveal the period of observation of the re-entering vehicle by the tracking system.

The data points for the curves of Figure 1 are derived from the conventional far-field equation:

$$P_r = \frac{P_t G_t G_r}{(4\pi)^2 R^2} \lambda^2$$

where P_t is the power transmitted, G_t is the transmitting antenna gain, G_r is the receiving antenna gain, λ the propagation wave length, and R the slant range. The range, being a function of time, permits the data to be plotted against this parameter.

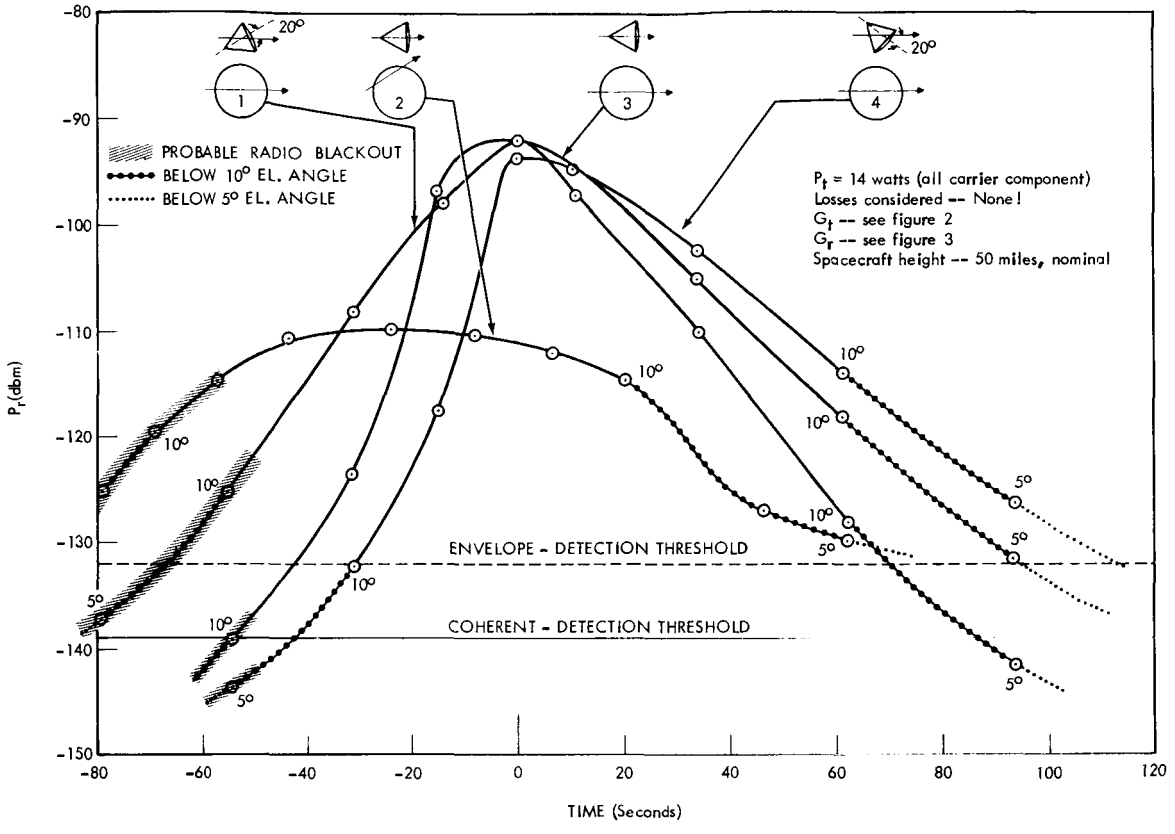

Figure 1–Re-entry Interferometer Received Signal Level

Proper interpretation of the Power received curves requires an examination of certain assumptions made in the values of some of the factors in the above equation. Principally, the spacecraft USB transmission characteristics are not established as yet, therefore these factors as well as others were assumed in these calculations.

SPACECRAFT TRANSMITTED POWER, P_t

Considerable uncertainty exists concerning the factors which influence the value of P_t. The latest estimate for the S-band power generated is 14 watts.[8] The estimated losses which account for the difference between the generated and transmitted power have a wide range depending upon the source of the information. The estimates for these losses range between about 2 db to as high as 10 db when considering that the antenna characteristics may be degraded by the rigors of the re-entry fire bath. Because of these uncertainties the value of the power transmitted is taken to be equal to 14 watts, the latest estimate for the power

generated. The power received curves can easily be juggled by the reader to account for his estimate of the losses by simply adding a constant factor to the power-received db scale.

It is assumed, that during re-entry, the auxiliary oscillator will be in operation which being incapable of modulation results in a pure carrier transmission.[9,11] This situation is beneficial to the interferometer in that under these conditions carrier lock-up will not be affected by sidebands, the possibility of spurious 500 cps signals generation is practically eliminated and the useable received signal power is maximized.

Although both the spacecraft and tracking propagation systems are right hand circularly polarized a polarization loss approaching 3 db will occur at particular orientations of the spacecraft and aspects to the ship.

SPACECRAFT S-BAND ANTENNA PATTERN, G_t

The spacecraft antenna pattern is also surrounded with uncertainties at this time. Although the Block I module (earth orbiting only) utilized scimitar antenna elements it appears that the Block II vehicle, used in return from the moon, will employ slot antennas. The performance interface specification for Block II has been modified recently to require that the S-band omni-directional antenna pattern have no nulls greater than -20 db except within 15° of the X axis. The null can be -24 db at 10° of the X axis. The coverage of 80 percent of the sphere should be not less than -3 db when operating with a right hand circularly polarized ground antenna. Since the actual pattern is not defined, the characteristics shown in Figure 2 were assumed. These follow approximately the above performance specification. The curve shown is the cross-section of the typical doughnut shaped spacecraft antenna pattern.

INTERFEROMETER SENSITIVITY AND ACCURACY[2,4,6]

The sensitivity of the re-entry tracker (see Appendix I) is determined to be -132 dbm in the open loop mode and -139 dbm in the closed loop mode. Open and closed loop refers to the type of demodulation in the receiver; open loop signifies conventional envelope detection which suffers a 7 db deterioration in the SNR at the prescribed threshold of the tracking system. Threshold is somewhat arbitrarily designated as that input signal level which results in an electrical phase noise jitter at the output of the final 3 cps post detection filter of 2° rms. Closed loop operation signifies coherent demodulation where phase lock techniques are used to extract an essentially noiseless carrier component which when multiplied

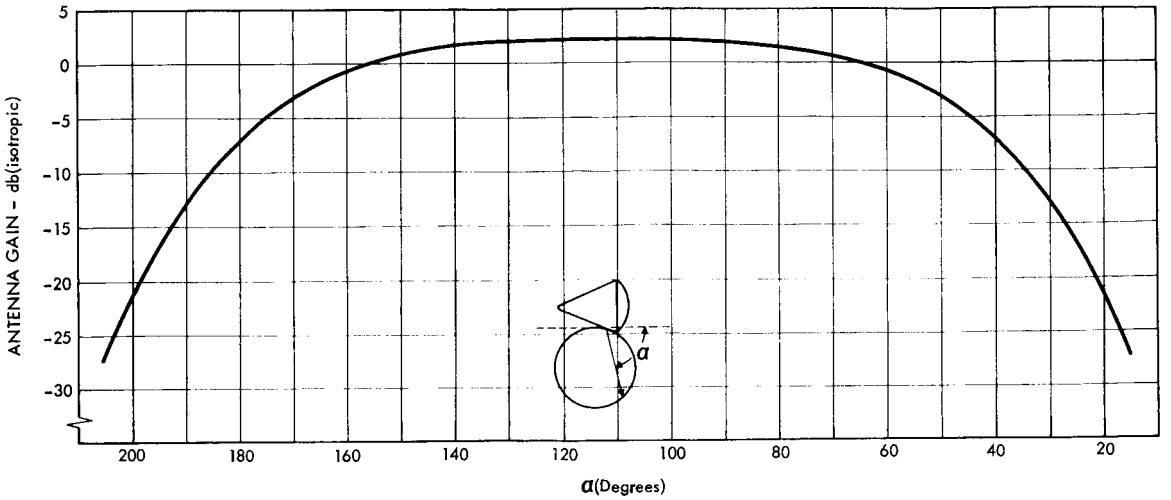

Figure 2–Assumed Command Module Antenna Pattern, Freq–USB

by the received signal plus noise results in demodulation with essentially no deterioration in the signal to noise ratio.

The accuracy of the interferometer proper, neglecting the errors due to antenna platform stabilization, ship torsions, etc., is calculated to have, at elevation angles of 10°, a peak value of very nearly 0.5° with a jitter due to thermal noise of 0.17° rms (Appendix II). The error due to imperfect antenna platform stabilization is specified to be a maximum of 0.25°. This will either be achieved through direct stabilization or suitable error readout devices which will correct the data in the az el conversion computer. Ship torsion errors are estimated to be 0.5° peak. The sum of these errors amounts to 1.25° peak with an rms jitter of 0.17°. With this system accuracy no difficulty should be experienced in acquiring the signal for the USB antenna with its 2.5° beamwidth. In addition, the method of computing the peak error is somewhat pessimistic since it is derived by the linear addition of eight errors all of which are of the slow drift type. Although the rms of these errors is felt to be far too optimistic, the probability that the peak sum will exist for a significant period is low indeed.

INTERFEROMETER ANTENNA PATTERN, G_r

The receiving antenna pattern is shown in Figure 3. This antenna ground plane assembly is composed of circularly polarized crossed slots with annular rings, functioning as surface-wave anti-phase suppressors arranged on the ground plane to reduce the horizontal propagation. These computed characteristics show a sharp drop off at elevation angles below 15°. The actual gain at low

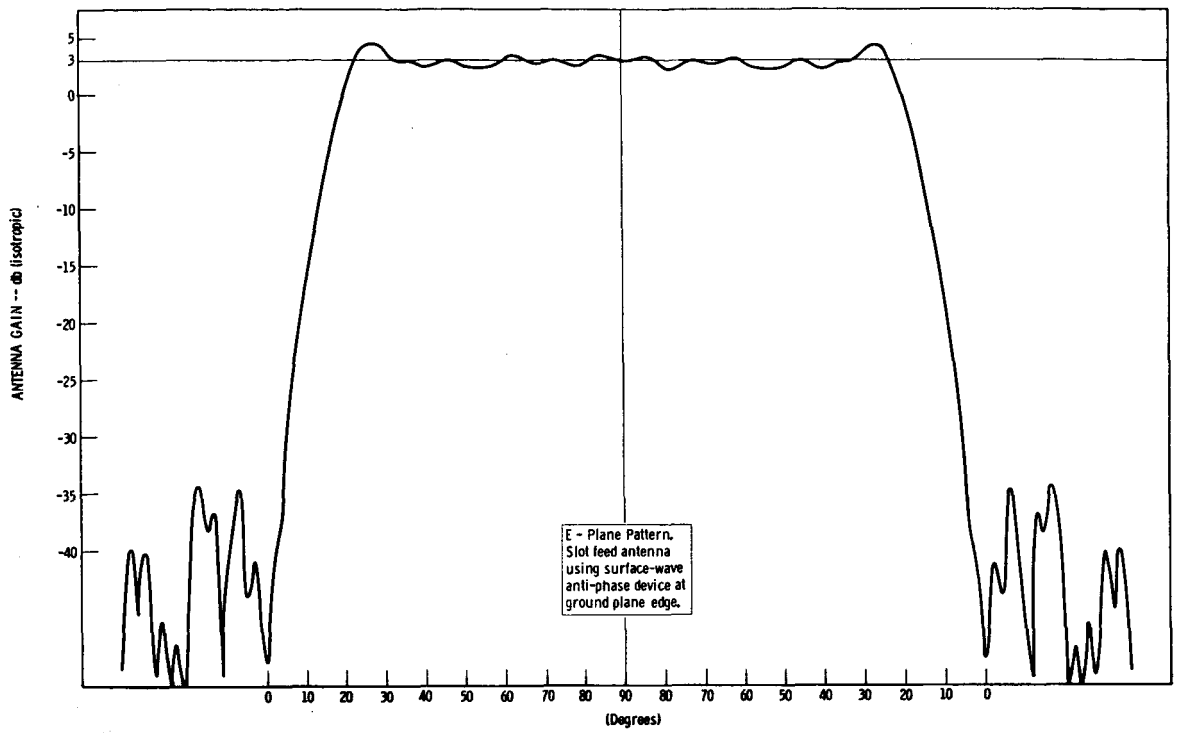

Figure 3–Interferometer Antenna Pattern

elevation angles will probably equal or exceed the values shown. This will be detrimental to sea return multipathing effects, but the theoretical model is probably too good in this respect.

TRAJECTORY GEOMETRY, (RANGE, ELEVATION ANGLES, TIME)

The trajectory geometry was extracted from the above cited report, X-513-64-85. Figure 4 is a simplified version of corresponding figures in the report. The trajectory parameters for all cases considered herein include reentry trajectories of 3000 nmi, lift to drag ratio of 0.5, and nominal spacecraft height of 50 nmi. Two trajectories are considered, directly overhead, and the one corresponding to the maximum lateral deviation. The spacecraft attitudes considered for the overhead trajectory are 20° lift, 20° drag, and horizontal. Spacecraft attitude variations for trajectories with a pronounced lateral deviation have essentially no effect on the received signal level, thus only the horizontal was investigated.

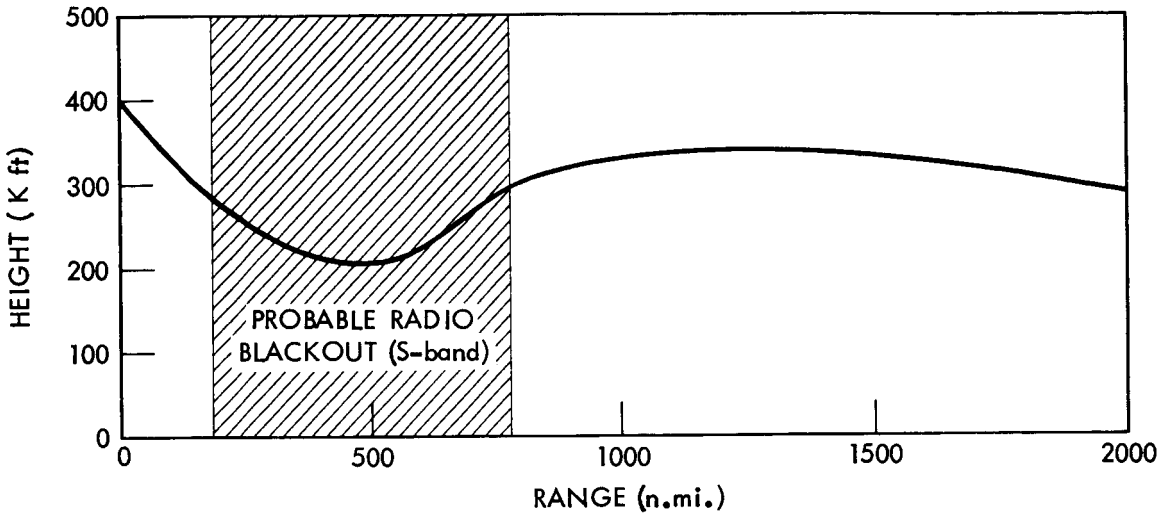

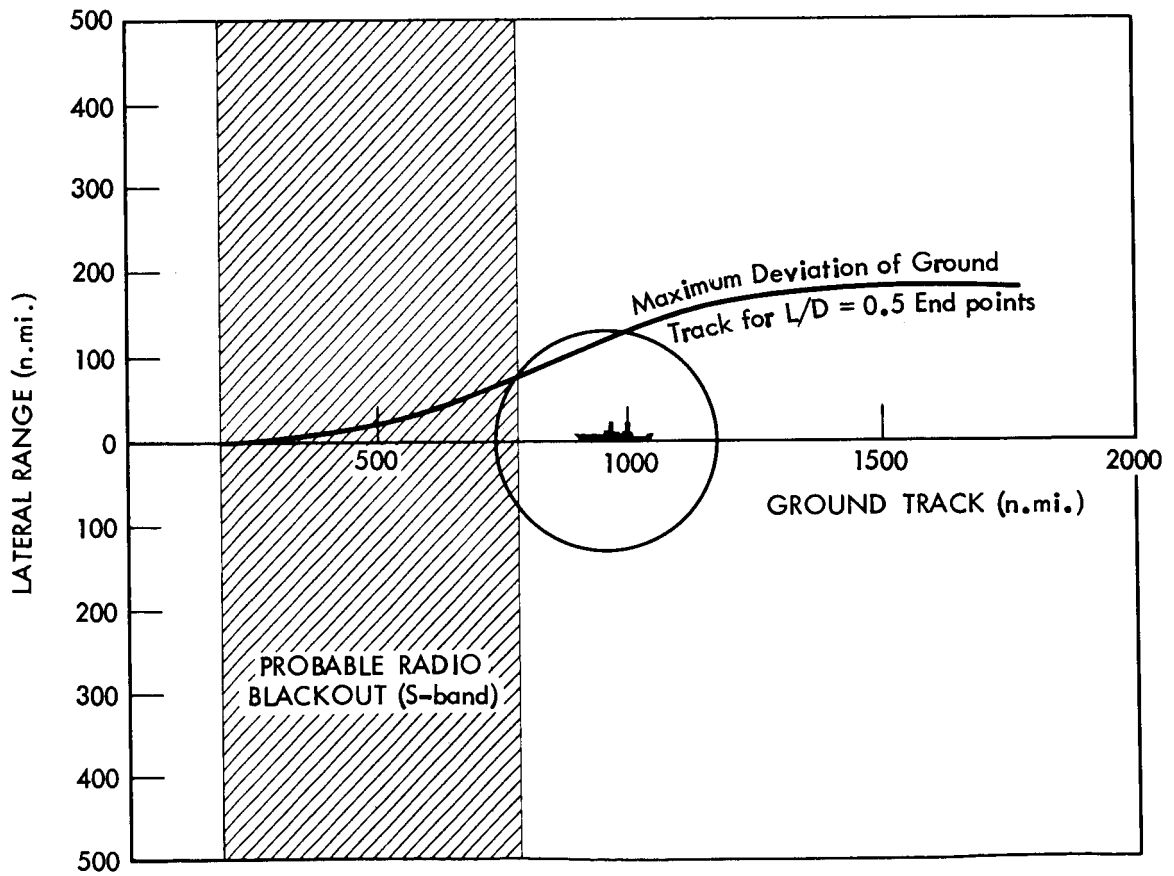

Figure 4–Apollo Re-entry Ground Tracks

RECEIVED SIGNAL LEVEL

To determine the variable factors in the far-field equation (G_t, G_r, R), it is necessary to derive the elevation and aspect angles as a function of Range. These angles, when plugged into the antenna response curves result in G_t and G_r. The angles and ranges were determined from a plot of the nominal 3000 kmi trajectory. These factors, in addition to the equation constants, permit the determination of the received signal power as a function of the trajectory geometry (or time as is desirable here). Zero, on the time scale, Figure 1, is arbitrarily chosen to correspond to interception by the spacecraft of a plane orthogonal to the overhead trajectory.

The data tabulated in Table 1 is derived from these curves. For the zero spacecraft loss case the total observation periods, T, is seen to be approximately 100 seconds for all except the maximum deviation trajectory which is 76 seconds. Fortunately, the T- value for this trajectory is 56 which should permit early acquisition of the USB signal.

Because of radio blackout limitations to the observation periods and the relatively steep skirts of the Power received curves the observation periods do not diminish appreciably in spite of rather severe losses introduced into the operation. For example, the data of Table 1 reveals that a loss of 10 db reduces the observation periods for the overhead trajectories by only about 10%. Furthermore, only until 20 db losses are introduced does the observation period for the maximum deviation trajectory show any decrease whatsoever.

CONCLUSIONS

Table 1 shows that signal acquisition can be established and pointing information supplied to the USB directive antenna with losses as high as 20 db introduced into the system. With a margin of this magnitude it is reasonable to expect satisfactory performance from the interferometer tracker as an acquisition aid even though several db's of the 20 db margin should properly be allocated to allow for degradation in the operational sensitivity of the interferometer per se.

It is important to recognize that the above margin corresponds to fully automatic operation of the tracking system; no operator manipulations whatsoever are required. A 7 db increase in sensitivity is obtained when phase lock-up, thus coherent demodulation, is achieved in the receiver. Frankly, neglecting this factor is being overly conservative since the lock-up is also fully automatic and with techniques now being perfected should be accomplished in less than 2 seconds after application of signal.

Table 1
Interferometer Tracker Observation Periods

T- Observational period before t = 0
T+ Observational period after t = 0
Observational periods are limited by elevation angles of 10°, Radio Blackout, or system threshold, whichever is less.
System threshold . . -132 dbm (non-coherent demodulator)

Geometry	Losses	T-	T+	T total
Overhead trajectory	0 db	42 sec	62 sec	104 sec
Horizontal Attitude	5	36	62	98
(Curve #3)	10	30	62	92
	15	26	60	86
	20	22	49	71
Overhead trajectory	0 db	50 sec	62 sec	112 sec
20° Drag	5	50	61	111
(Curve #1)	10	50	52	102
	15	43	45	88
	20	36	37	73
Overhead trajectory	0 db	31 sec	62 sec	93 sec
20° Lift	5	25	62	87
(Curve #4)	10	19	62	81
	15	15	62	77
	20	11	57	68
Maximum Lateral	0 db	56 sec	20 sec	76 sec
Deviation trajectory	5	56	20	76
Horizontal Attitude	10	56	20	76
(Curve #2)	15	56	20	76
	20	48	6	56

REFERENCES

1. Vonbun, F. O., "Re-entry Tracking for Apollo", GSFC report X-513-64-85, March 6, 1964

2. Simas, V. R., "A System for Re-entry Tracking of the Apollo Spacecraft", GSFC report X-523-63-56, April 2, 1963

3. Mengel, J. T., et al, "Application of Radio Phase-Comparison Techniques to the Study of Atmospheric and Rocket-Flame Refraction", NRL Report 4598, 1955

4. Simas, V. R. et al, "Re-entry Tracking System Development", GSFC Quarterly report I-230-63-19, pp. 11-47, Sept. 1964

5. Byrd, S. S., "Re-Entry Tracking for Apollo", GSFC report X-512-65-146, March 29, 1965

6. **Taylor, R. E. et al, "Design Analysis of the GSFC Apollo Re-entry Tracking System", To be published.**

7. **Woodman, et al,** "Phase Measurement/Display Subsystem for the Apollo Re-entry Tracking System", GSFC report X-531-63-251, December 13, 1963.

8. North American Document, "GOSS Interface report ground operational support System" SID 63-881, Revised July 15, 1964

9. North American Document, "Apollo Spacecraft GOSS Communications circuit margins", SID 62-1452, September 1963

10. Wiack, R. J., "Phase Measurement/Display System Operations and Maintenance Manual", GSFC Report X-523-65-256, March 1965

11. North American Document, "The Second Interim Report, Apollo Modulation Technique Study", Sept. 3, 1963

12. Silberberg, R., North American Document No. PM-64-59, December 22, 1964

APPENDIX I

INTERFEROMETER TRACKER SENSITIVITY

Although customary to express the sensitivity of receiving systems in terms of the output SNR as a function of the input signal level it is more meaningful to denote the interferometer tracker sensitivity in terms of the output phase noise. The methods are equivalent, however, since the interferometer output signal level is a constant, i.e., it is merely the voltage that corresponds to 360° of phase.

There are several considerations which effect the selection of system threshold criteria in terms of the standard deviation of the electrical phase noise variations, σ_ϕ. The basic consideration is the required space-angle accuracy which is determined to be 1.25°. This value is set by the 1.25° half beamwidth of the USB antenna for which the interferometer tracker serves as an acquisition aid. In view of the peak errors involved with the mount stabilization and ship flexture factors, which cannot be materially reduced without the expenditure of considerable money and effort, the error budget allocated to receiver and sky thermal noise is necessarily a relatively small part of the total 1.25°. In addition, the ambiguity resolving requirement of the 10 to 1 baseline step as well as receiver dynamic range problems caused by the necessary high I.F. noise levels are factors which determine the threshold level. In considering all of the factors one quickly "zero's in" on about 2° rms as an appropriate noise level criteria for threshold. The ambiguity and dynamic range problems are appropriately satisfied, and the standard deviation of the space angular variations, σ_θ, at elevation angles of 10° is 0.17° – a suitable value for threshold.

ENVELOPE DETECTION

The relationship between the phase noise and input signal level for an interferometer of this type using an envelope detector (Reference 3):

$$\sigma_\phi = \left(\frac{N_1}{P_r}\right)^{1/2} \left(2 + \frac{N_2}{P_r}\right)^{1/2} \qquad (1)$$

where

$N_1 = K B_1 (T_R + T_S)$

$N_2 = K B_2 (T_R + T_S)$

B_1 is the post detection passband = 3 cps

B_2 is the predetection passband = 200 kc

T_R is the effective noise temperature of the receiver = 175°

T_S is the sky noise integrated over the hemisphere and weighted by the antenna gain = 12°

Thus: $N_1 = 1.38 \times 10^{-23} \times 3\ (175° + 12°) = -171$ dbm

$N_2 = 1.38 \times 10^{-23} \times 2 \times 10^5\ (175° + 12°) = -123$ dbm

Letting $\sigma_\theta = 2°$ rms = -14.5 db radian,

$P_r = -132$ dbm (Envelope detector threshold).

To avoid a messy quadratic equation, the above value for P_r is obtained iteratively. To show that $P_r = -132$ dbm is correct it can be substituted into equation 1 and the value of σ_θ checked for agreement with -14.5 db radian.

$$\sigma_\theta = \left(\frac{N_1}{P_r}\right)^{1/2} \left(2 + \frac{N_2}{P_r}\right)^{1/2}$$

$$\left(\frac{N_1}{P_r}\right)^{1/2} = \frac{-171 \text{ dbm} - (-132 \text{ dbm})}{2}$$

$$= -19.5 \text{ db}$$

$$\frac{N_2}{P_r} = -123 \text{ dbm} - (-132 \text{ dbm})$$

$$= 9 \text{ db}$$

$$\left(2 + \frac{N_2}{P_r}\right)^{1/2} = \sqrt{10} = 5 \text{ db}$$

Thus $\sigma_\theta = -19.5$ db + 5 db = -14.5 db, which shows the desired agreement.

COHERENT DETECTION

The coherent detector removes the effect of the predetection passband term from the equation for phase noise resulting in:

$$\sigma_\theta = \left(2\frac{N_1}{P_r}\right)^{1/2} \tag{2}$$

Setting this expression equal to the same phase variation as before results in:

$$P_r = \frac{2N_1}{\sigma_\theta^2}$$

= 3 db -171 dbm + 2 × 14.5 db radians

= -139 dbm (Coherent detector threshold).

APPENDIX II

INTERFEROMETER TRACKER ACCURACY

Since the objective of the interferometer tracker is to track the spacecraft radiated signal with sufficient accuracy to allow the USB 2.5° beamwidth dish to lock on, the required system accuracy is about 1.25°. This total error must be budgeted between a number of system error sources:

Interferometer receiving and data processing system phase drifts

Antenna alignment and phase center variations

System phase variations from receiver and sky noise

Antenna platform stabilization errors

Ship flexture angular uncertainties.

In deriving an error budget an assessment must be made of the above errors and their relationship to cost of reducing. The error budget was established following mainly the principle of minimizing system developmental, production and operating costs.

RECEIVER AND SKY ADDITIVE NOISE ERRORS

The threshold of the interferometer system has been established in Appendix I as 2° electrical phase deviation. The system angular resolution for the interferometer is related to the electrical phase noise as follows:

$$\cos \theta = \frac{\phi}{B}$$

where θ is the space angle, ϕ is electrical angle measured by the interferometer and B is the baseline distance thus:

$$\sigma_\theta = \frac{\sigma_\phi}{B \sin \theta} \text{ cycles} = \frac{\sigma_\phi}{360\, B \sin \theta} \text{ space degrees.}$$

Letting σ_ϕ = 2° rms, B = 10.5 wavelengths and the elevation angle, θ = 10°,

$$\sigma_\theta = \frac{2}{360 \times 10.5 \times 0.175} = 0.003 \text{ radians}$$

$$= 0.17° \text{ rms}$$

INTERFEROMETER SYSTEM PHASE DRIFTS, $\Delta\phi$

Transmission lines	0.5°
Front End	0.5°
I.F. and detector	0.5°
Phase detector	0.2°
Signal processing	0.1°
D/A synchro converter	0.2°
	2.0° total

Through the relationship between interferometer phase and space angle the system phase drifts correspond to $\Delta\theta$ = 0.17°. This error as well as all system errors except for the additive noise fluctuations is considered a slowly varying peak error. As discussed previously, one is tempted to derive the total drift error as the rms; however, the duration of some of these errors and the fact that they might not in all cases be independent leads to the more pessimistic technique of combining them according to linear addition.

ANTENNA PHASE CENTER VARIATIONS

The 0.5 db ripple, δ_{db} in the antenna characteristics, Figure 3, is caused by spurious phasors induced by the edge effects of the ground screen. The corresponding electrical phase variations, $\Delta\phi$, are derived as follows:

$$\Delta\phi = \left(\log^{-1}\frac{db}{20}\right) - 1 \text{ radians.}$$

$$= 0.06 \text{ radians} = 3.4°$$

then $\Delta\theta$ at 10° elevation angles, through the preceding interferometer relationships, is 0.3°.

TOTAL ERROR

The drift errors are listed as follows:

Error Source	Error – $\Delta\theta$
Interferometer phase drifts	0.17°
Antenna phase center variations	0.3°
Antenna platform stabilization errors	0.25°
Ship flexture angular uncertainty	0.5°
Total	1.22° $\approx$ 1.25°

Receiver and sky additive noise fluctuations . . . 0.17°rms

It is considered appropriate to view the system accuracy as a peak drift of 1.25° carrying an rms jitter, in a 3 cps pass band, of 0.17°. It is important to note that this accuracy corresponds to elevation angles of 10°; the accuracy is better by approximately a factor of six overhead.